Indian Journal of Marine Sciences
Vol. 39 (2), June 2010, pp. 165-181

Oil spill model based on the kelvin wave theory and artificial wind field for the Persian Gulf

M A Badri* & A R Azimian**

Department of Mechanical Engineering, Isfahan University of Technology, Iran
[E-mail: *malbdr@cc.iut.ac.ir, **azimian@cc.iut.ac.ir]

Received 20 February 2009; revised 16 June 2009

Oil spill simulation due to the wind and wave fields and tidal currents in the Persian Gulf by solution of the hydrodynamics and convection-diffusion equations have been presumed. Model consists of algorithms describing the processes of advection, surface spreading, horizontal and vertical dispersion, evaporation and emulsification. Tidal constituents have been obtained from co-tidal charts. Sea level and surface velocity has been determined by Kelvin Wave theory as a new hydrodynamic calibration tool to prepare flow pattern and successful speed-up procedure. Artificial wind field has been generated in order to prepare wind field time series in the accident interval. Performance of the hydrodynamic model for tidal currents in the Persian Gulf is examined and tested using measurement results by imposing tidal fluctuations to the main open boundary at the Hurmoz strait. The spill analysis model was setup using the flow field produced by the hydrodynamic model to simulate an accidental oil spill and its performance was further validated using the existing data at the Kish Island. Langevin equation for vertical dispersion has been calibrated for the considered domain. Comparison of the actual and simulated oil spill drift was found reasonably acceptable allowing for application in risk assessment analysis in the northern part of the Iranian waters.

[**Keywords:** Oil spill modelling, Kelvin wave theory, Artificial wind field, Persian Gulf]

Introduction

A number of oil spill models have been developed since 1960's[1]. Most of these models are essentially transport models or limited to two dimensional hydrodynamic models with fate analysis, mainly dealing with surface spreading[2,3]. A comprehensive oil spill model should consist of a set of algorithms to simulate the fate and transport of oil in three dimensions including spreading, advection, turbulent diffusion, evaporation, dispersion, dissolution, photo-oxidation, biodegradation and sinking/sedimentation[4,5,6].

A major part of an oil spill can contaminate shorelines and causes a long-term damage to the aquatic environment for fishery, wildlife, harbor facilities, vessels and health of mankind. Therefore, many government agencies have prepared oil spill contingency plans. One of the important components of these plans is to use the mathematical models to predict transport and fate of oil slicks[7]. Generally, transport and fate of the spilled oil can be affected by physical, chemical and biological processes. Both Eulerian and Lagrangian descriptions are used to determine pollutant dynamics in a continuous media. For Eulerian co-ordinates, calculations are carried out in fixed grid points for some specific moments of time based on the classic advective-diffusion equation. It is practically impossible to detect exactly the oil spill boundaries in a specific moment by the solution of the turbulent advective-diffusion equation. Moreover, turbulent diffusion in the form of the Boussinesq's K-theory has very simplified physics. The solution of this problem is more appropriately expressed by the Lagrangian co-ordinate system, which relates to the positions of numerous individual particles. These particles, in their collective form, determine distribution relationships[8]. Some extensive studies related to the oil spill have been published[9,10,11]. It appears that oil drop entrainment from the surface oil film to the water column is an important mechanism, because it uniquely serves to remove the oil from the surface without any changes in the physical or chemical properties in contrast to evaporation and emulsification[12,13]. Considering the importance of these processes in the mathematical expression of dispersion in oil spill models, a three-dimensional model of oil dispersion is presented for the Persian Gulf. This model is based on Kelvin

* Assistant Professor
** Professor

propagation wave theory as a new hydrodynamic model. The Lagrangian description has been used to describe horizontal and vertical movement and oil dispersion using a calibration technique on the horizontal and vertical dispersion coefficients and Langevin equation.

Materials and Methods

Preparing the supporting parameters for the model

In this work, some of the important short-term processes have been considered and a portal has been provided to be used in a developed numerical model. Weather data in the interval of the accident were prepared and imposed to the hydrodynamic model to simulate the trajectory, surface oil slick and thickness. An artificial wind field has been generated and calibrated by means of data from the European Center for Medium–Range Weather Forecast (ECMWF) or data from Iranian synoptic stations with fairly good conformity (Table 1). This field has been imposed by means of a vortex flow or storm [14]. The center point of the storm has been initially set at the north-west corner of the Persian Gulf, latitude: 30 00 N, longitude: 48 00 E by considering the followings:

- Velocity of storm in both x and y direction is 0.25 [degree/hr]
- Storm center pressure is 3.5 [bar]
- Maximum radius of storm is 25,000 [m]

The total data has been generated for the oil spill interval and the maximum velocity at the largest radius has been determined as 3.67 [m/sec] to generate mean prevailing Persian Gulf wind field (Fig. 1). To compare the wind data, Cressman analysis has been used as well. The wind velocity and direction have been extended to the grid points considering the curvature of the earth using the following:

$$r_{i,j} = \cos^{-1}\left[\begin{matrix}\sin(glat)\times\sin(slat)+\cos(glat)\times\cos(slat)\\ \times\cos(glon-slon)\end{matrix}\right]\times earthradius \quad (1)$$

Where $r_{i,j}$ is the distance between two points s (synoptic stations) and g (grid points), *lat* and *lon* are latitude and longitude of points respectively. Therefore the value of wind velocity has been calculated for the grid points as follows:

$$F_g = \{\sum_{i=1}^{n}\sum_{j=1}^{m}(W_{i,j}\times F_o)/\sum_{i=1}^{n}\sum_{j=1}^{m}W_{i,j}\,W_{i,j} = \max\{0,(R^2-r_{i,j}^2)/(R^2+r_{i,j}^2)\}\} \quad (2)$$

Where F_o is the data in m stations, F_g is the value of data in n grid points, R is influence radius and $W_{i,j}$ is the weight function of the stations related to the grid points.

For the sun-earth-moon system, there are so many tide-raising-force constituents. A number of 15 are related to lunar, 7 to solar and the rest are related to long-period and shallow water. Among these constituents such as diurnal, semi-diurnal, third-diurnal, fourth-diurnal, sixth-diurnal and long-term, four main constituents have been selected as below:

- Semi-diurnal M_2 for the moon and S_2 for the sun, periods of 12.42 [hr] and 12.00 [hr] respectively
- Diurnal K_1 and O_1 both for the moon, periods of 23.93 [hr] and 25.85 [hr] respectively

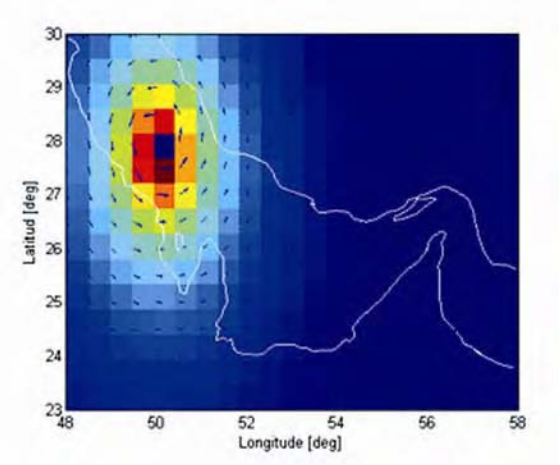

Fig 1a—Typical artificial wind at Persian Gulf location-1 hr

Table 1—Comparison of wind velocity by Cressman analysis, artificial wind field and NOAA data

Item	Lat.	Lon.	NOAA	Cressman	Error (%)	Artificial wind field	Error (%)
1	28.00	51.00	1.47	1.350	8.6	1.79	17.8
2	27.50	51.00	1.72	1.362	20.8	1.72	0.0
3	27.00	50.00	1.58	1.336	15.4	1.38	14.5
4	27.00	52.00	1.70	1.167	31.0	2.12	19.8
5	26.50	51.00	1.72	1.371	20.3	1.56	10.2
6	26.50	53.00	1.73	1.027	40.6	2.37	27.0

Mostly, other constituents have small amplitudes and often are not considerable. The weight of other constituents is about 1.5-2% and is ignored here. In this work, four main constituents have been considered by using Admiralty method of tidal prediction NP 159-1969[15]. The surface level has been determined using the following equation for the Persian Gulf by considering seasonal streams:

$$ML = M_2 + S_2 + K_1 + O_1 + 0.15 \quad (3)$$

These parameters have been calculated for all grid points and are compared with the available data at four different locations i.e. Kish and Siri islands and Bandar abbas and Bushehr ports for validation (Table 2). Meanwhile, using these constituents and Kelvin Wave theory, the water surface level and water surface velocity have been calculated. In this study, Persian Gulf is considered as a shallow water basin considering its overall latitude at $\phi = 27^{\circ}$. Shallow water intermediate range $0.7 \prec kh \prec 3.0$ is considered. The kh parameter which is usually introduced to measure the depth strength, shows that the Persian Gulf has the condition of a shallow water (mean kh is calculated about 0.95 in the Persian Gulf). Where k is the wave number modulus and h is mean depth[16]. Due to the influence of the Coriolis force, the direction of the wind drift vector is turned relatively to the wind direction. Tidal propagating Kelvin wave model for a 35 [m] mean depth has been considered. The deviation angle θ_{dev}, turns to the right on the northern hemisphere which is fitted for the Persian Gulf (Fig. 2a). In this work, it is assumed that [17]:

$$\theta_{dev} = \beta_w.\exp\{\ \alpha_w |U_{wind-10m}|^3/(g.\upsilon_w)\ \} \quad (4)$$

Where $\alpha_w = -0.3\times10^{-8}$ and $\beta_w = 12°30'$. The magnitude of the wind drift angle varies with the geographical location and wind speed. In this proper situation, the Persian Gulf is located in the direction towards the water surface drift and can be assumed as a channel (Fig. 2b). In rigid boundaries, velocity in y-direction must vanish, which implies:

$$\partial^2\eta/\partial y.\partial t - f.\partial\eta/\partial x = 0,\ y = 0, L \quad (5)$$

Where f is coriolis factor ($f = 2\Omega.\sin\phi$), Ω is the angular velocity of earth and ϕ is the latitude. Therefore, the governing equation for η becomes:

$$\frac{\partial}{\partial t}\{(\partial^2/\partial t^2 + f^2)\eta - C_0^2\nabla^2\eta\} = 0 \quad (6)$$

Wave solutions which are periodic in x and t can be sought in the following form:

$$\eta = \mathrm{Re}\,\overline{\eta}(y)\,e^{i(kx-\sigma t)} \quad (7)$$

Where $\overline{\eta}(y)$ is the complex wave amplitude which varies with the cross-basin coordinate y. Substitution of (7) into (5) yields an eigen value problem for $\overline{\eta}$. The general solution will be:

$$\overline{\eta} = A\sin\alpha y + B\cos\alpha y \quad (8)$$

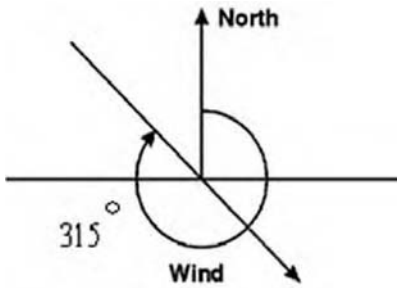

Fig. 2a—Prevailing wind direction in Persian Gulf

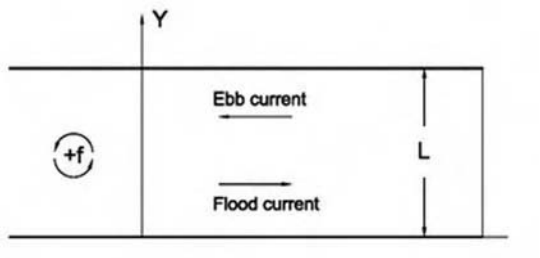

Fig. 2b—Infinite basin of width L rotating with angular velocity f/2

Table 2—Comparison of tidal constituents for 4 locations in the Persian Gulf

Tidal constituents	M2		S2		K1		O1		ML
	Amp.	Ph	Amp.	Ph.	Amp.	Ph.	Ph.	Amp.	
Max. Error %	14.1	15.2	27.5	21.1	18.4	19.8	20.7	23.4	18.9
Min. Error %	0.0	0.6	3.6	1.3	1.8	0.9	2.9	2.9	1.3

Table 3—Phase of constituents by normalizing of constituents based on minimum phase

Item	Station	Water Depth [m]	kh	Lat.	Lon.	M2 [Deg.]	S2 [Deg.]	K1 [Deg.]	O1 [Deg.]
1	Bandar Abbas	20	0.75	27°13′*N*	56°22′*E*	5.600	6.261	1.250	1.000
2	Kish Island	29	0.90	26°30′*N*	53°59′*E*	1.000	1.991	4.152	2.831
3	Siri Island	76	1.50	25°53′*N*	54°29′*E*	1.000	4.902	13.638	9.305
4	Bushehr Port	13	0.60	28°54′*N*	50°49′*E*	1.000	1.210	1.224	1.035

Table 4—Amplitude of constituents by normalizing of constituents based on maximum amplitude

Item	Station	Water Depth [m]	kh	Lat.	Lon.	M2 [m]	S2 [m]	K1 [m]	O1 [m]
1	Bandar Abbas	20	0.75	27°13′*N*	56°22′*E*	1.000	0.300	0.312	0.200
2	Kish Island	29	0.90	26°30′*N*	53°59′*E*	1.000	0.400	0.951	0.571
3	Siri Island	76	1.50	25°53′*N*	54°29′*E*	1.000	0.353	0.752	0.483
4	Bushehr Port	13	0.60	28°54′*N*	50°49′*E*	1.000	0.422	0.938	0.622

Using boundary conditions at y=0 & y=L yields two linear homogeneous equations for A and B. Therefore, the eigen value relation yields:

$$(\sigma^2 - f^2)(\sigma^2 - C_0^2 k^2)\sin \alpha L = 0 \quad (9).$$

When $\sigma^2 = C_0^2 k^2$, the solution plays the role of n=0 mode due to the effects of the rotation and is named Kelvin Wave. By considering the solution which propagates in the positive x-direction:

$$\alpha^2 = -f^2 / C_0^2 \quad , \alpha = \pm if / C_0 \quad (10)$$

By assuming $\alpha = if / C_o$ without loss of generality, it is possible to write the dynamic field as follows:

$$\eta = \eta_0 e^{-fy/C_0} \cos(k[x - C_0 t] + \varphi) \quad (11)$$

$$u = (\eta_0 / h).C_0 \, e^{-fy/C_0} \cos(k[x - C_0 t] + \varphi) = -(g / f)(\partial \eta / \partial y) \quad (12)$$

$$v = 0 \quad (13)$$

Where η is Kelvin wave height, η_0 wave amplitude, $C_0 = \sqrt{g \cdot h}$ wave propagation velocity, y distance from the boundary wall, $\sigma = C_0 k$ wave angular frequency, φ phase, x distance from the origin, h mean height of the Persian Gulf. In this work, stream velocity affected by tidal stream has been calculated by superposition of the main constituents M_2 , S_2 , K_1 and O_1 .

$$\eta_{water\ surface\ level} = \sum_{j=1}^{4} [\eta_{0j} . e^{-fy/C_0} \cos(kx - \sigma t + \varphi_j)] \quad (14)$$
$$\text{j: used for } M_2, S_2, K_1 \& O_1$$

$$u_{tidal\ stream} = \sum_{j=1}^{4} [(\eta_{0j} C_0 / h) . e^{-fy/C_0} \cos(kx - \sigma t + \varphi_j)] \quad (15)$$
$$\text{j: used for } M_2, S_2, K_1 \& O_1$$

Where η_{0j} and φ_j are amplitude and phase of the main constituents respectively. Water surface level (WSL) and water surface velocity (WSV) in the time interval of the oil spilling, 25th April-10th May 2007 have been calculated regarding the Kelvin wave theory and artificial wind field. It is determined by means of an in-house program as a simple and applicable estimation especially for the Persian Gulf situation. The results for WSL and WSV have been compared to the Admiralty tide tables and measurements respectively with good conformity (Figs. 3-b, c). To show the Kelvin wave theory application, the amplitude and phase of the main constituents have been determined by normalizing of each constituent and inserting in the relations (14, 15) based on the maximum amplitude and minimum phase (Tables 3 and 4). Results have been compared for four mentioned locations. For Kish and Siri Islands and Bandar Abbas port the kh parameter is laid in the intermediate range. For these locations, WSL and WSV have fair agreement with hydrodynamic model. In Bushehr port, kh parameter is calculated below 0.7 where the strong nonlinear effects are important. As expected, for this location WSL and WSV do not have fair agreement. Vertical velocity component, w in the z direction has been determined by a Logarithmic profile:

$$w(z) = U_f . \ln[30(h - z) / k_n], U_f = \{ V_{mean} . \kappa / [\ln(30h / k_n) - 1] \} \quad (16)$$

Where z is the vertical coordinate measured from the sea surface, w(z) is the logarithmic current profile and κ is von Kármán's constant (0.42). h is water

depth and k_n is Nikuradse roughness factor. U_f is friction velocity and V_{mean} is the mean current velocity and based on Kelvin wave theory is $\sqrt{u^2+v^2} \approx u$.

A hydrodynamic model for Iranian Waters

Some test problems, have been considered to determine the flow patterns and also to validate and initiate the main problem design. These test problems are simple channel, expansion and contraction channels and channel with an open boundary similar to the real domain (i.e. the Persian Gulf). The boundary conditions are as follows:

- Inflow (left entrance) and open boundary; fluctuation time series in water surface level similar to tidal stream variations
- Outflow (right exit); uniform velocity

In these sample problems, some of the results such as the flow pattern (velocity field) and the particle trajectory are presented. An oil spill accident has been assumed for simulation purposes in a proper time interval. Boundary conditions have been set for solid and open boundaries. By means of Admiralty tide tables, the fluctuations of the water surface elevation have been imposed for time interval at Hurmoz strait as open boundary. The coast lines and islands of the Persian Gulf are considered as the boundaries of the flow domain. At these boundaries the component of the normal velocities are set to zero. Hydrodynamic modeling of the Persian Gulf was first conducted to provide the flow field needed for oil spill modeling. This model has been simulated as unsteady flow using unstructured grid system with 7288 nodes and 13532 elements. The model takes into account density variations, bathymetry and external forcing such as meteorology, tidal elevations, currents and other conditions. It applies the classical Navier-stocks equations for mass and momentum conservation in three dimensions. The hydrodynamic model is dynamically coupled with the temperature and salinity modules, which are resolved by advection–dispersion processes. The turbulent fluctuations are modeled employing the Boussinesq eddy viscosity concept and the $k-\varepsilon$ turbulence closure. The tidal rising forces and the density force create prominent axial flow and a northern anticlockwise current develops a west flowing current from the Straits of Hurmoz along the Iranian coast. This has been already shown in a typical open boundary test problem (Fig. 4-b). In terms of wind effect, a NW to SE wind field was found to develop the current along the Iranian coast. Therefore, a prevailing wind with a monthly-averaged velocity of 5.25 [m/sec] and direction 315[$^\circ$] has been used to calibrate the artificial wind field.

The described hydrodynamic model is used to compute flow patterns in the Persian Gulf using unstructured mesh due to:

- The tidal fluctuations at east boundary (open boundary) and river inflow at west coast
- The evaporations from water surface and emulsification to the water column
- The friction and irregularities of coasts and bed

In order to verify performance of the model and the quality of the results, the tidal fluctuations at Didamar Island, obtained from Admiralty tide table for the period of 15 days, are imposed at Hurmoz strait at the east open-end of the flow domain (Fig. 3a).

Model Description

In the Lagrangian discrete particle algorithm, the oil slick is divided into a large number of small grids

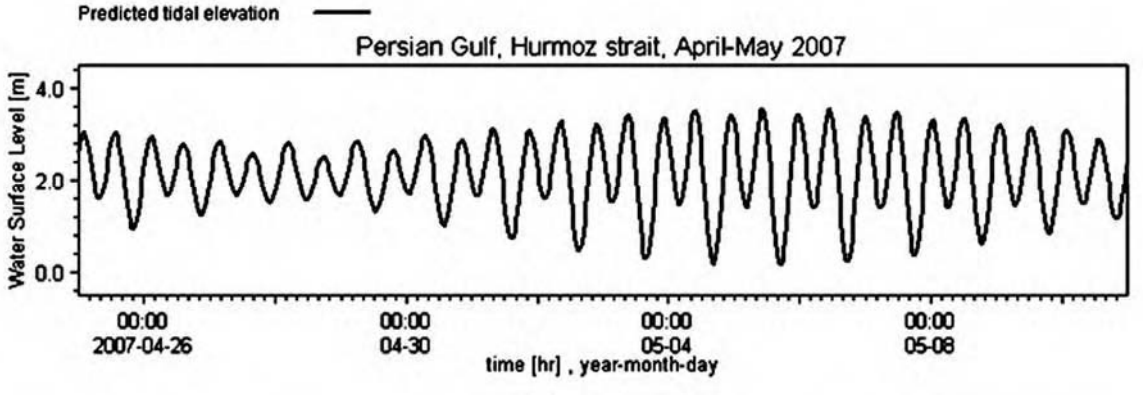

Fig. 3a—Water surface level fluctuations imposed at open flow boundary (Hurmoz strait)

and a set of plane coordinates are assigned to each grid. These particles are introduced into the sea at a rate corresponding to the oil spilling rate. In this model, the initial oil slick area is divided into small grids and the advection properties of each grid have been computed. After computing the velocity and displacement of each point, the shape and track of the oil slick can be determined. The total volume of the spilled oil on the sea surface has been characterized by the number N of infinitesimal particles under the influence of:

- The regular movement of the media with the velocity components $u(x,y,z,t)$, $v(x,y,z,t)$ and $w(x,y,z,t)$
- The turbulent fluctuations, $u'(x,y,z,t)$, $v'(x,y,z,t)$ and $w'(x,y,z,t)$

The co-ordinates X_k, Y_k and Z_k of particles in x, y, z directions can be determined as follows:

$$\frac{dX_k}{dt} = u + u'_k \;,\; X_k = X_k^0 + (u + u'_k).\Delta t \tag{17}$$

$$\frac{dY_k}{dt} = v + v'_k \approx v'_k,\; Y_k = Y_k^0 + (v + v'_k).\Delta t \approx Y_k^0 + v'_k.\Delta t \tag{18}$$

$$\frac{dZ_k}{dt} = w + w'_k + w_b,\; Z_k = Z_k^0 + (w + w'_k + w_b).\Delta t \tag{19}$$

Where u, v, w are determined from the hydrodynamic model for each time interval t. In general, w_b depends on the size of the particle k. The component of the oil drop emergence w_b and the droplet size are estimated by assuming the particle to be spherical and rigid and applying the force balance between the buoyancy and drag forces[18,19,20].

$$w_b = g.d_k^2.\Delta\rho/(18\mu_w), d_k = 9.52\mu_w^{2/3}/(g.\rho_w.\Delta\rho)^{1/3} \tag{20}$$

Where g is the gravity, ρ_o and ρ_w are oil and water density respectively and $\Delta\rho$ is density difference. μ_w is the water dynamic viscosity. Velocity fluctuations u'_k, v'_k and w'_k can be calculated based on the random walk technique.

Spreading and Advection

In this study, using trajectory-model, surface oil slick spreading has been calculated as[5]:

$$\frac{dA_k}{dt} = C_k A_k^{0.33}(h_k)^{1.33} thick - slick \;\&\; \frac{dA_t}{dt} = C_{1t} A_t^{0.33}.\left[-C_{2t}/(h_t + 0.00001)\right] thin - slick \tag{21}$$

where A_k and A_t represent the area of thick and thin oil slick respectively. Also, h_k and h_t stand for thick and thin oil slick thickness respectively. Drift velocity of the surface oil is usually considered to be a vector sum of a wind induced drift and a water-current drift. Therefore, the drift velocity of the surface oil is presented as a vectorial addition. Displacement of each point has been calculated based on the displacement velocity $\vec{U}(U_x, U_y)$ due to the wind and wave fields and tidal stream. Advective velocity or total drift velocity, $\vec{U}$ for every point, can be calculated as follows:

$$\vec{U} = k_t \vec{U}_{tide} + k_w(z).(\vec{U}_{wind} + \vec{U}_{wave}) \tag{22}$$

Where $\vec{U}_{wind}$ and $\vec{U}_{wave}$ are wind and wave induced velocities respectively. Also $(\vec{U}_{wind} + \vec{U}_{wave})$ has been determined based on the wind velocity at 10 meters above the sea level.

$$\vec{U} = k_t \vec{U}_{tide} + k_w(z).\vec{U}_{wind-10m} \tag{23}$$

Where $\vec{U}_{tide}$ is depth integrated current velocity, k_t is advective water current factor which has been set for the Persian Gulf as 1.0. Also $k_w(z)$ is the wind drift considering the Persian Gulf based on a parabolic vertical profile $k_w(z) = k_w^*(1 - 3z/h).(1 - z/h), 0 \le z \le h$. Where h is the local water depth, z is the vertical particle co-ordinate, measured from the sea surface and k_w^* is the wind drift factor which has been selected 0.026 by Wave Model (WAM). This parabolic profile causes the wind-generated flow in the upper third of the water column to be in the same direction as the current and the flow in the lower part to be in the opposite direction of the wind matching the physical condition of the Persian Gulf.

Horizontal and Vertical Dispersion

Although viscosity has some effect on the rate of the spreading, the dominant physicochemical parameters of the crude oil that determine spreading are density and dispersion coefficients. The velocity fluctuations u'_k, v'_k and w'_k are normally calculated by random walk procedure [21].

$$u'_k = V'_h.[R]_0^{+1}.\cos(2\pi[R]_0^{+1}) \quad (24)$$

$$v'_k = V'_h.[R]_0^{+1}.\sin(2\pi[R]_0^{+1}) \quad (25)$$

$$w'_k = V'_v.(2[R]_0^{+1} - 1.0) \quad (26)$$

$$V'_h = \sqrt{c_h D_h / \Delta t}\ , V'_v = \sqrt{c_v D_v / \Delta t} \quad (27)$$

Where V'_h and V'_v are stochastic turbulent fluctuations for horizontal and vertical movements respectively. Also D_h and D_v are horizontal and vertical diffusion coefficients respectively and $[R]_0^{+1}$ is referred to a probability density with a mean of 0 and a standard deviation of 1. The directional angle is assumed to be a uniformly distributed random angle ranging between 0 and 2π, that is $2\pi[R]_0^{+1}$. The diffusion step size S is generated randomly by $S = [R]_0^{+1} S_{rms}$, Where $S_{rms} = \sqrt{4D_h.\Delta t}$ is the root mean square distance. Also c_h and c_v have been selected 12 and 6 respectively. So, the distance any grid point moves by horizontal and vertical diffusion s_h and s_v or horizontal and vertical transport of the parcel[10] are:

$$s_h = [R]_0^{+1}\sqrt{12D_h\Delta t}\ ,\ S_v = (2[R]_0^{+1} - 1.0)\sqrt{6D_v\Delta t} \quad (28)$$

Where D_h and D_v have been set up for the Persian Gulf as:

$$D_h = (1/16).C_{Dh}.\pi.k_h^2.\left[\Delta.g.V^2/\mu_w^{1/2}\right]^{1/3}.(1/\sqrt{t}) \quad (29)$$

$$D_v = 0.028\ C_{Dv}.(H_s^2/T_w)e^{-2k.z} \quad (30)$$

$$H_s = 0.243U_{wind-10m}^2/g, T_w = 8.13U_{wind-10m}/g \quad (31)$$

Where $\Delta = (\rho_w - \rho_o)/\rho_o$, H_s is the wave height, T_w is the wave period and k is the wave number (2π/wave length). C_{Dh} & C_{Dv} are the horizontal and vertical diffusion coefficient correction factors. These correction factors are determined by means of calibration respectively and z is the vertical coordinate of the oil droplets. The displacement of the kth parcel after a time step Δt for N parcels of the oil spill is:

$$X_k = X_k^0 + u.\Delta t + [R]_0^{+1}.\sqrt{12D_h.\Delta t}\ \cos(2\pi[R]_0^{+1}) \quad (32)$$

$$Y_k = Y_k^0 + [R]_0^{+1}.\sqrt{12D_h.\Delta t}\ \sin(2\pi[R]_0^{+1}) \quad (33)$$

$$Z_k = Z_k^0 + w\Delta t + \left(2[R]_0^{+1} - 1.0\right)\sqrt{6D_v.\Delta t} + 5.04\left[(\Delta\rho.g.\mu_w)^{1/3}/\rho_w^{2/3}\right].\Delta t \quad (34)$$

where the initial coordinates of the kth parcel are X_k^0, Y_k^0, Z_k^0. The buoyancy force depends on the density and size of the droplet and the vertical velocity w has been used from the basic physical processes such as tides, winds and waves which essentially provide 3D currents[22]. The oil droplets move in response to the current shear (advection), turbulence (diffusion) and buoyancy[23]. For investigation and validation of the vertical oil dispersion, the Langevin equation has been considered [24]:

$$\frac{dw'_k}{dt} = -\beta w'_k(t) + \gamma.[R]_0^{+1} \quad (35)$$

Where β and γ are the coefficients representing the covariance $w'_k(0).w'_k(t)$ and energy dissipation rate $w'^2_k(t)$ respectively. Based on the results, β and γ can be determined by considering a best fit to vertical velocity fluctuation:

$$w'_k(t) = (1/\beta)\left[\gamma.[R]_0^{+1} - \exp(-\beta.t)\right] = 0.022\exp(-1.64t) \quad (36)$$

To calibrate the mean value of β and γ for the Persian Gulf, it is found that the covariance $w'_k(0).w'_k(t)$ and dissipation rate $w'^2_k(t)$ are proportional to 1.64 and $0.22[R]_0^{+1}$ respectively. It is worth mentioning that, in a similar research, the researcher did not consider emulsification and dissolution [24].

Oil Decay by Evaporation, Emulsification and Dissolution

In this work, the volume fraction of the oil evaporated is determined by a single component theory relation[23]:

$$F_{ev} = (\alpha_{ev}/C).[\ln P_0 + \ln(C.K_E.t + 1/P_0] \quad (37)$$

Where F_{ev} is volume fraction of evaporation, α_{ev} is a correction coefficient, P_0 is initial vapor pressure at

temperature T_E, k_E is $0.0025U_{wind-10m}^{0.78}A.\upsilon/(R.T.V_0)$ and T is temperature of oil. V_0 is initial spill volume, υ is molar volume, R is gas constant, C and T_0 have been calculated based on their relations to oil Index(API) and t is time.

Some of oil components can also dissolve into the water column from a surface slick. In the present study, the method of Cohen[25] is used to take into account these components. In this method, F_{dis} is the rate of dissolution for the slick, K_d is a dissolution mass transfer coefficient and A is the area of the oil slick.

$$F_{dis} = k_d A S_0.\exp(-\beta_{dis}.t) \tag{38}$$

Where $S_0.\exp(-\beta_{dis}.t)$ the oil solubility in water[26], S_0 is fresh oil solubility and β_{dis} is a decay constant. Under the influence of the wave action, water droplets may become entrained into the oil slick to form water-in-oil emulsions. Here, the change in water content with time can be expressed as [27,28,29,30,31]:

$$\ln\left[(1-K_2F_{em}).\exp\{-2.5F_{em}/(1-K_1F_{em})\}\right] = -3.43\times10^{-5}U_{wind-10m}^2.t \tag{39}$$

Where F_{em} is the rate of emulsification or water content fraction of the emulsion for the slick, K_1 and K_2 are constant rate for water incorporation and a constant rate depending on coalescing tendency.

Results

A semi stochastic oil spill model is built. The model employs surface spreading, advection, evaporation, emulsification and dissolution algorithms to determine transport and fate at the surface. The water current drift has been obtained by two different hydrodynamic calibrations. Horizontal and vertical dispersions are simulated by random walk procedures. The slick transportations over the water surface and in the water column is due to the balance between gravitational, viscous and surface tension forces, wind and wave fields and tidal stream effects. Evaporation and emulsification have been considered as decay dominant components.

The portal contains wind velocity and direction, wave height and period, tidal main constituents, water surface level and tidal stream. Some of the important parameters have been validated by measurements. Table 1, compares the wind velocities calculated by an artificial wind field and Cressman analysis with NOAA data at some typical points at the spillage interval displaying fairly good conformity. The minimum error was in the northern part of the Persian Gulf with 8.6 % and the maximum error was in the southern part of the Gulf. The maximum error is due to the lack of data near Arabian countries. Hence, artificial wind field has been used not only because of the smaller amount of mean deviations on the whole grids, but also because of the possibility of the time series generated. Table 2, compares the calculations and measurements of the main tidal constituents and water surface level ML in four different locations such as Kish and Siri islands and Bandar abbas and Bushehr ports. To justify the hydrodynamic models, calculations of time history for water surface level and surface layer currents near Kish Island have been compared to the measured data. Figs. 3b and 3c show the comparison of the measured data and the Kelvin wave theory calculation results.

The trajectory of particles in arbitrary locations for one of the test problems in 6 hours durations are shown in Fig 4a, b. It presents an axial flow anticlockwise current develops a west flow from the open boundary similar to the Persian Gulf. Water surface drift velocities in the middle of the channels are compared in Figs 5a, b. Flow surface velocity in an expansion channel is about 3 times more than a contraction one. Also, flow surface velocity in a simple channel is about 10 times more than a limited channel with an open boundary like the Persian Gulf. Hence, it is predictable that the advection of particles/oils in the Persian Gulf would be less than a basin with inflows and outflows such as a simple channel. Figs 5.c,d,e show the effects of wind, water surface level fluctuations and salinity on water surface velocity for a short term 6 hours simulation at the Persian Gulf. As shown, water surface level fluctuations have more effects than wind field and salinity effect. Hence, in this work more attention has been paid to generate a tidal stream since the oil spill trajectory should be more sensitive to tide and tidal stream. Computed water levels at Kish Island (Latitude: 27 13 N and Longitude: 56 22 E) is compared with measured values obtained from Iranian Hydrography center (Fig. 6-a) in the corresponding time which is an interval of two weeks from 25 April-10 May 2007. The comparison period was chosen based on the actual available measured

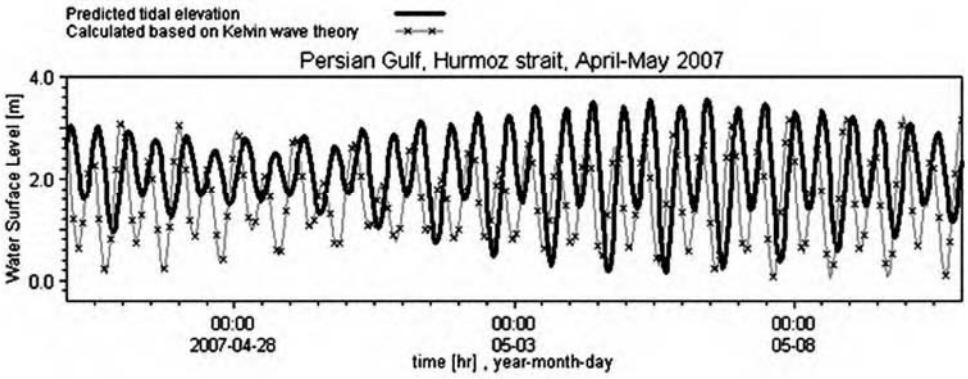

Fig. 3b—Comparison of computed Kelvin wave theory and predicted tidal elevation at open boundary

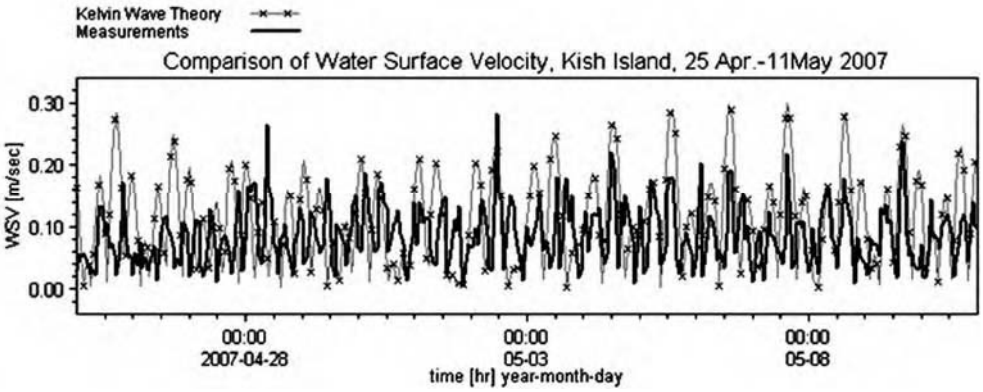

Fig. 3c—Measured and computed water surface velocity

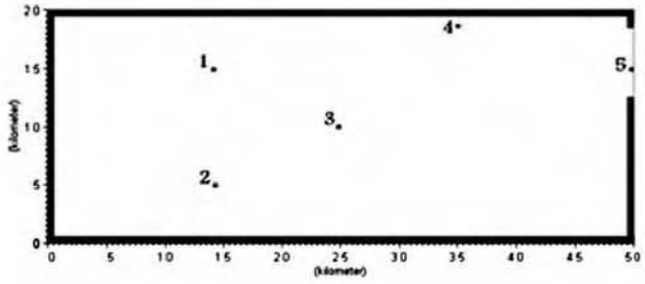

Fig. 4a—Typical particles in an open boundary channel

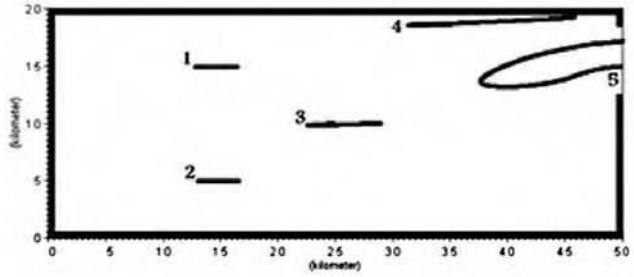

Fig. 4b—Trajectory of particles in an open channel

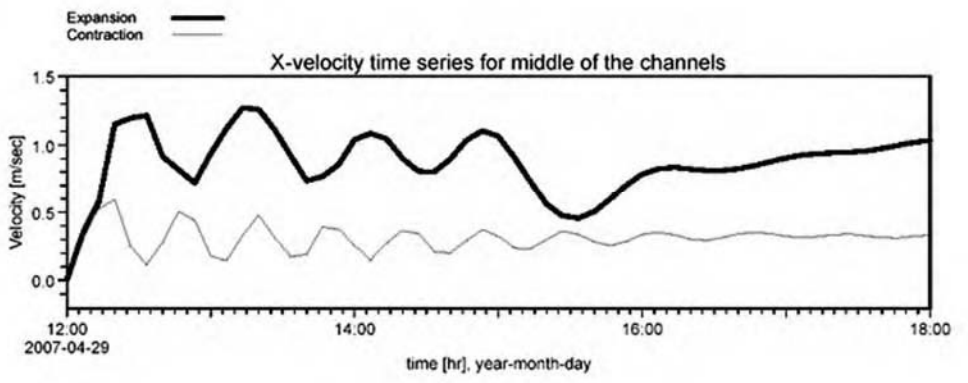

Fig. 5a—Comparison of water surface drift velocity time series for expansion & contraction channels

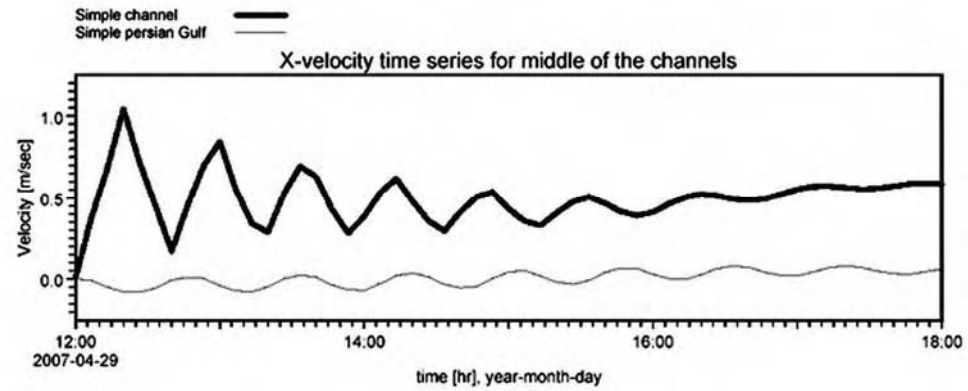

Fig. 5b—Comparison of water surface drift velocity time series for a simple & an open boundary channel

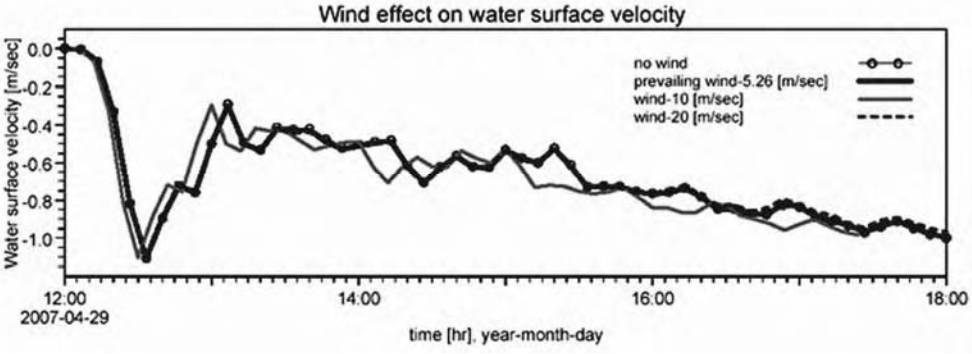

Fig. 5c—Wind effect on water surface velocity at the Persian Gulf

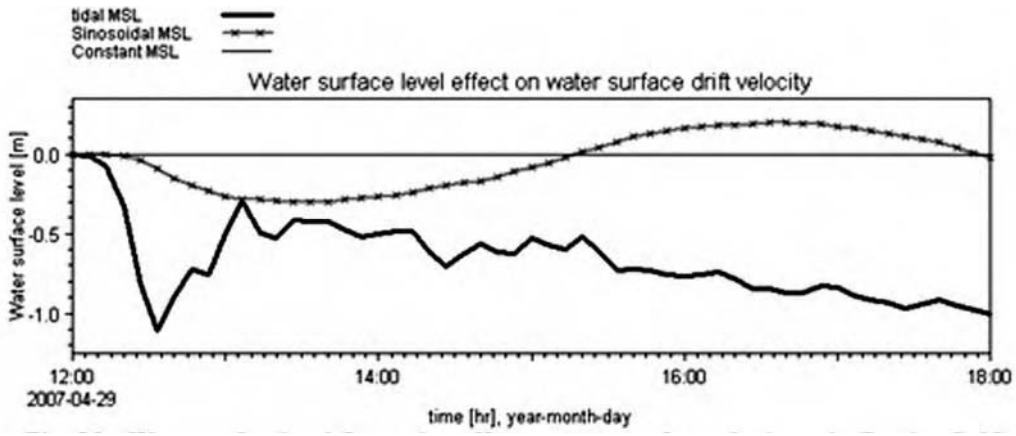

Fig. 5d—Water surface level fluctuation effect on water surface velocity at the Persian Gulf

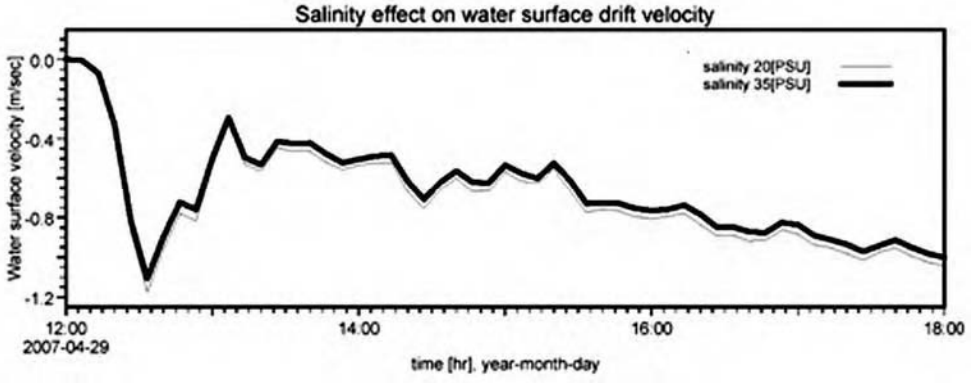

Fig. 5e—Salinity effect on water surface velocity at the Persian Gulf

data time periods. A set of data from a current meter at the depth of 10 m near the Kish Island were available. For the comparison of the averaged currents (Fig. 6-b), the same time interval April-May 2007 is selected. They show fair agreement between measurement data and predicted results obtained from another hydrodynamic model.

In Fig. 7, measured and computed water surface velocities for two hydrodynamic models are compared. In fact the difference between water surface velocities determined by hydrodynamic model, Kelvin wave theory and measurements are compared to each other based on measurement data. It shows that the results from the Kelvin wave theory, especially for the Persian Gulf based on its proper geometrical situation, is about 3 times better than the hydrodynamic model. Maximum time index is referred to 1.5 days duration. Moreover, CPU time

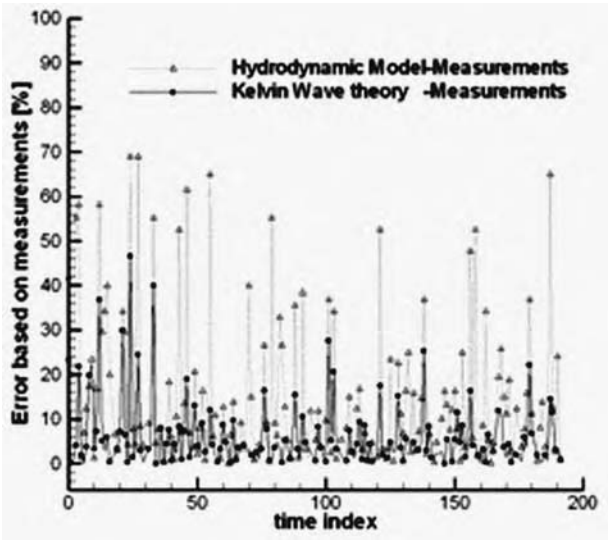

Fig. 7—Comparison of water surface velocity

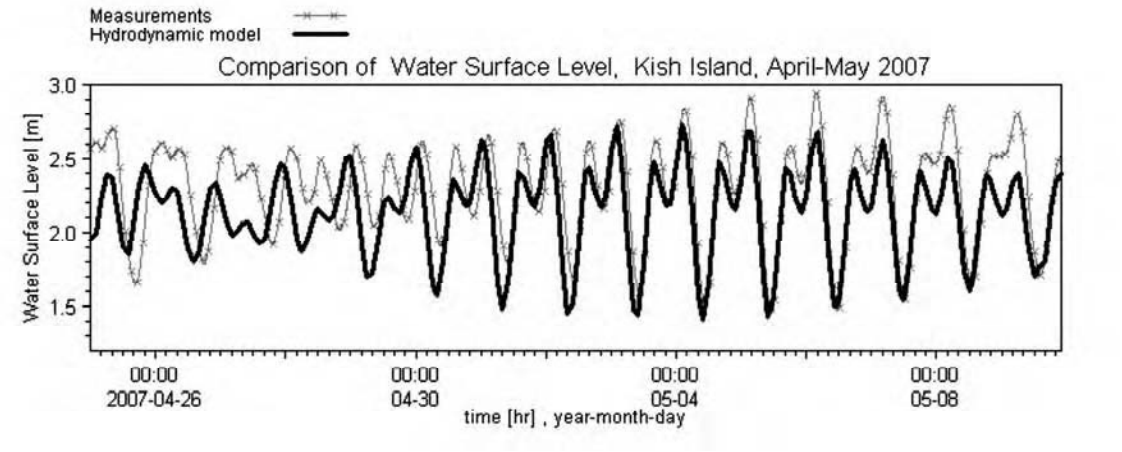

Fig. 6a—Comparison of computed and measured water surface level near Kish Island

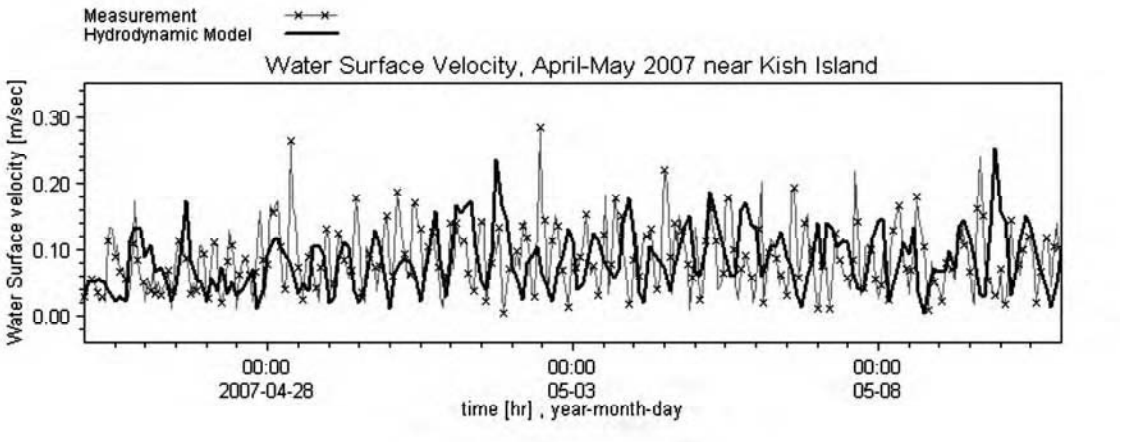

Fig. 6b—Comparison of computed and measured water surface velocity

for the hydrodynamic model was estimated about 4.5-8 hours per one run-time based on the time step selection in comparison with about 1.5 min for the Kelvin wave theory which presents a successful speed-up procedure. These two models are compared (Figs. 8a, b) for water surface level and water surface velocity. As shown in the second half of the time interval, two time series follow each other. In the first-half of the time interval, hydrodynamic model spends warming up period. An average flow is presented in Fig. 9 for simulation conditions with mean water current drift about 20 [cm/s]. The predicted average surface flow pattern well agrees with the known flow pattern features of the Persian Gulf[10].

Determination procedure of C_{Dh} & C_{Dv} in a case study, is shown in Figs (10-a, b). As it can be seen, the horizontal and vertical dispersion coefficients are calibrated as 3 and 0.015 near Kish Island in order to have a best conformity to water surface velocity. Time series of horizontal dispersion coefficient and variation of the vertical dispersion coefficient versus water depth before and after corrections for the Persian Gulf are shown in Figs (10-c, d). These Figures are introduced by

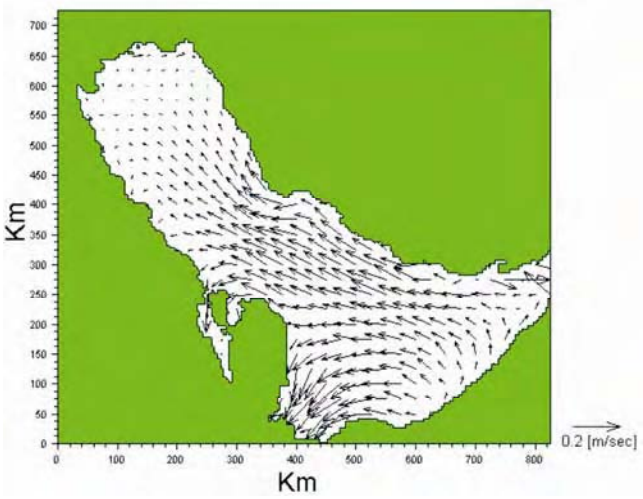

Fig. 9—Average flow for simulation time interval

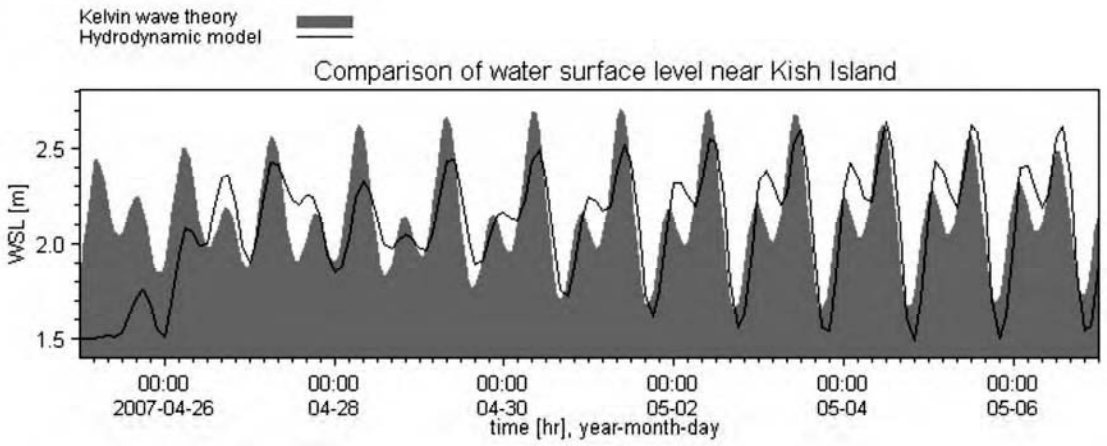

Fig. 8a—Comparison of water surface level for two hydrodynamic model near Kish Island

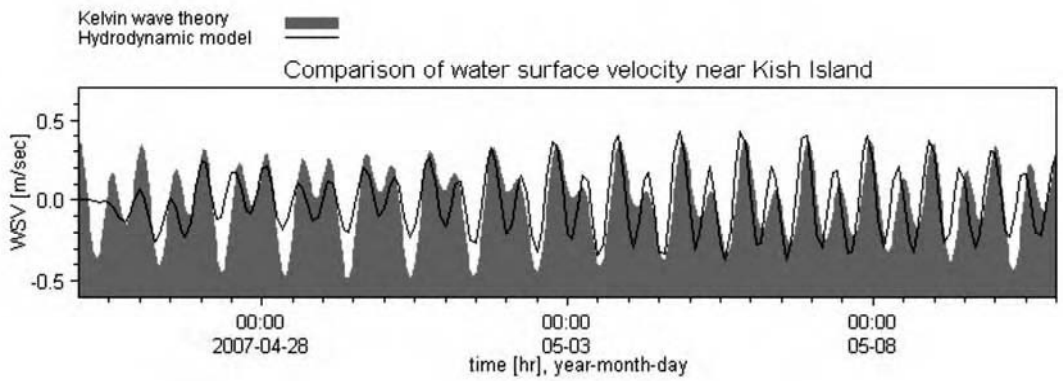

Fig. 8b—Comparison of water surface velocity for two hydrodynamic model near Kish Island

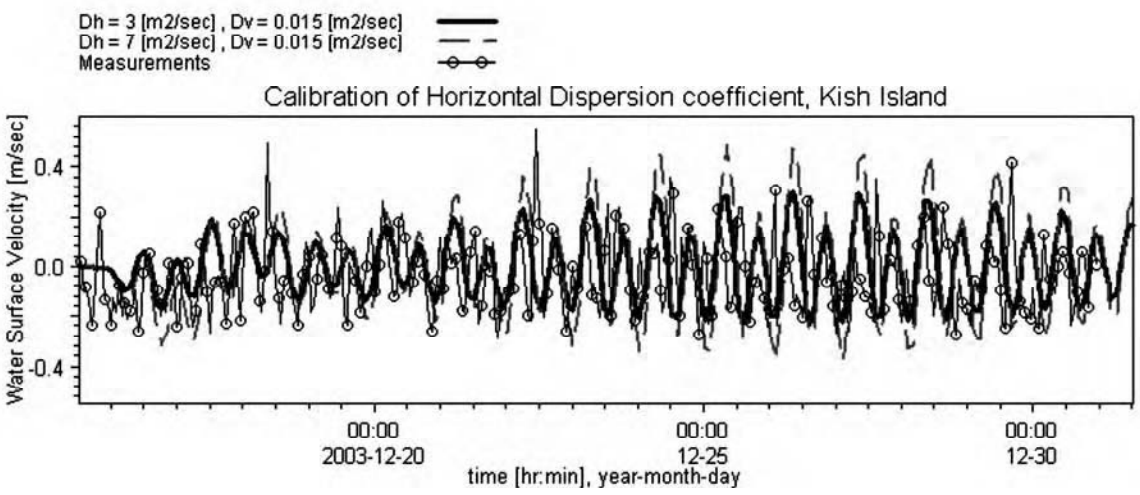

Fig. 10a—Calibration of horizontal dispersion coeff. near Kish Island

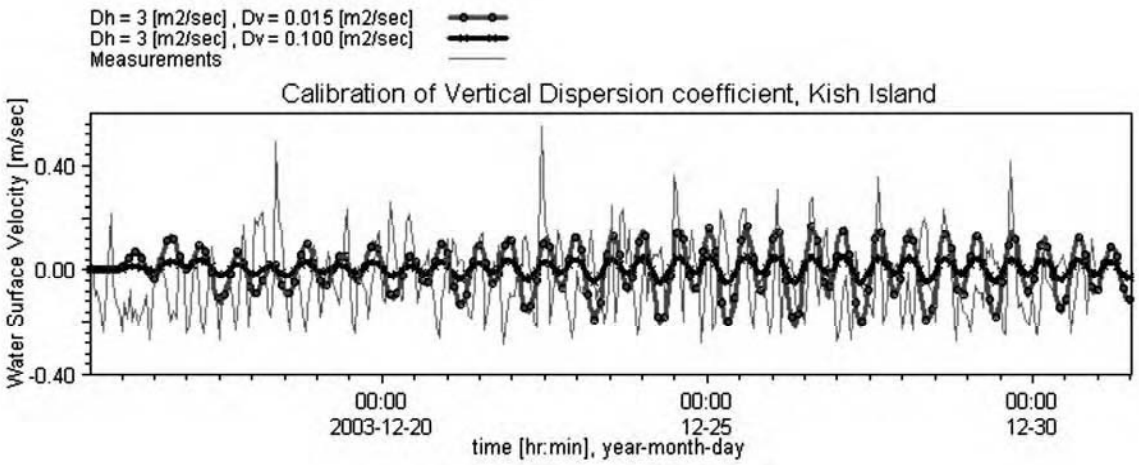

Fig. 10b—Calibration of vertical dispersion coeff. near Kish Island

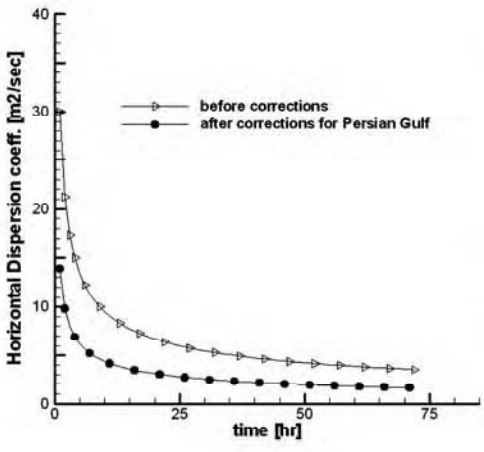

Fig. 10c—Time series of horizontal dispersion coeff.

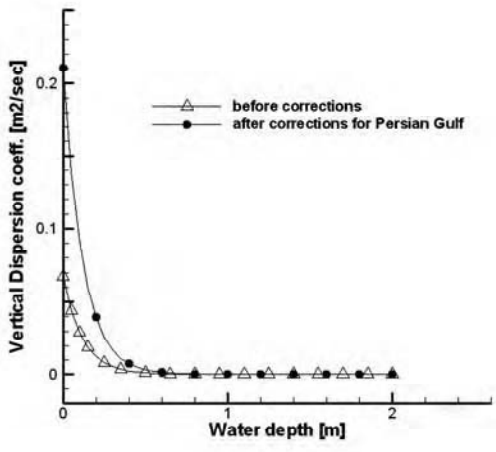

Fig. 10d—Variation of vertical dispersion coeff.

means of the correction factors C_{Dh} & C_{Dv} as 0.463 and 3.15 respectively to calibrate the relations 29 and 30. Where

$$D_h = 0.0289\pi k_h^2 \left[\Delta g.V^2/\mu_w^{1/2}\right]^{1/3}.(1/\sqrt{t}) \;\&$$
$$D_v = 0.088(H_s^2/T_w).e^{-2k.z}.$$

Typical trajectories by consideration of both water drift velocity $\vec{U}(u,v,w)$ and fluctuation components $\vec{U}'(u,v,w)$ for 6 hours duration are shown in Figs. 11-a, b. It is worth mentioning that the oil spreading pattern is the same but displacement in an expansion channel and simple channel are about more than 3 times than a contraction and open boundary channel respectively. Also, oil spill spreading near Kish island and Bandar Abbas port in a real condition in the Persian Gulf for 15 days duration are shown in Figs. 12-a, b. Based on the flow patterns, the oil spreading near these locations are somehow greater than the other locations, because these points are located near the Hurmoz strait which is an open boundary. In Fig. 13 the constant coefficient C_k for surface spreading has been set up and calibrated as $C_k = 6.20$ during 72 hours for the Persian Gulf near Kish Island.

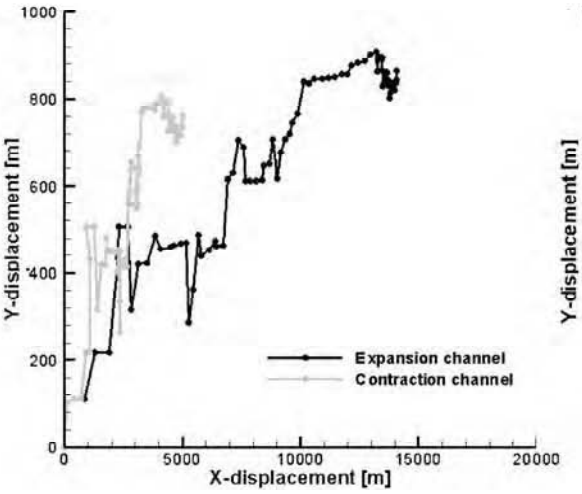

Fig. 11a—Comparison of oil trajectory for contraction and expansion channels

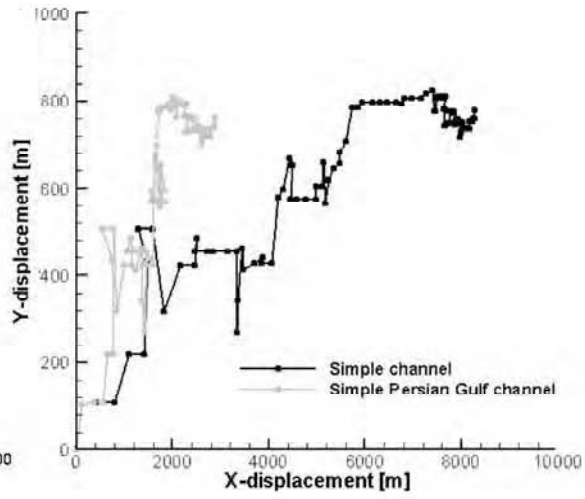

Fig. 11b—Comparison of oil trajectory for simple channel and open boundary channel

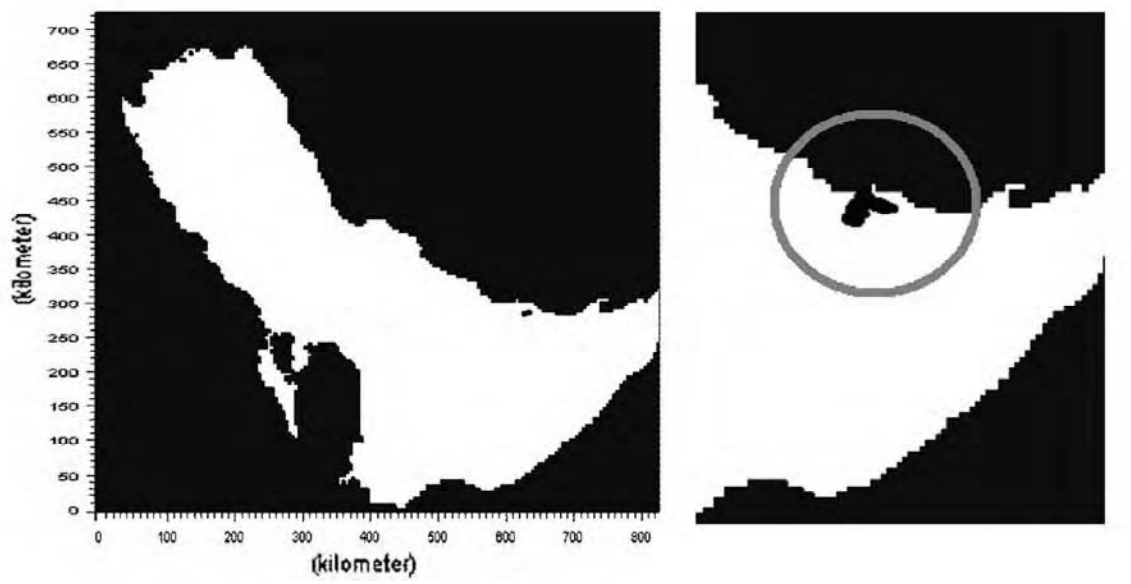

Fig. 12a—Typical oil spill locations (left), trajectory after 15 days (right) near Kish Island

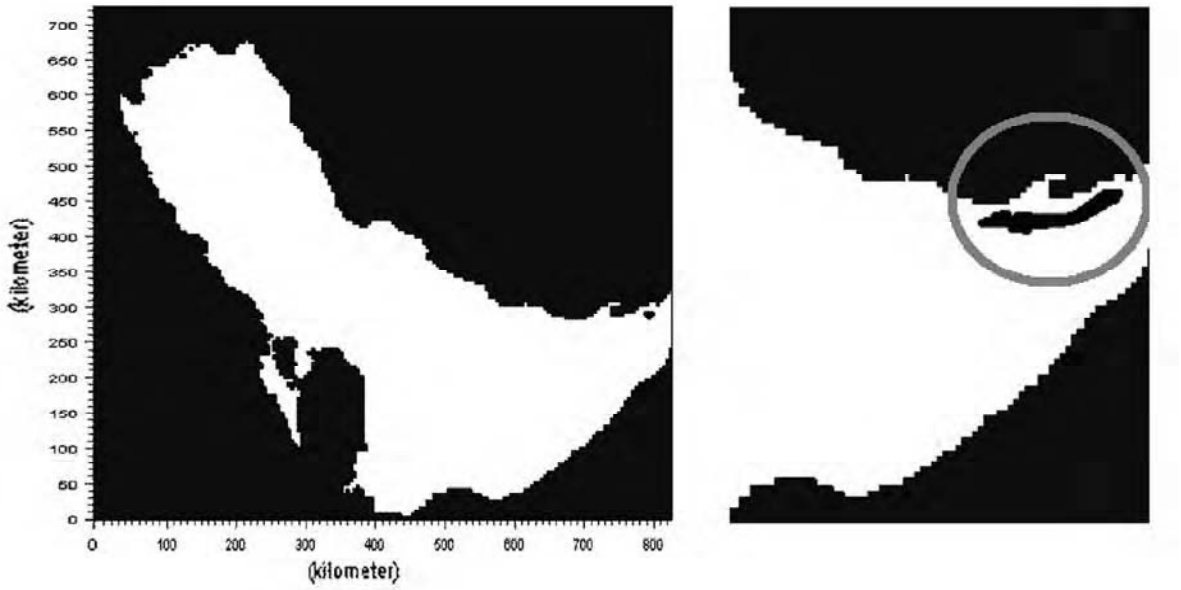

Fig. 12b—Typical oil spill locations (left), trajectory after 15 days (right) near Bandar Abbas port

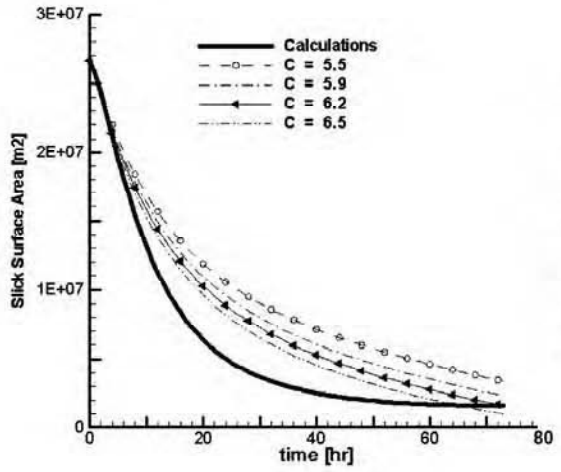

Fig. 13—Calibration of oil slick area coeff.

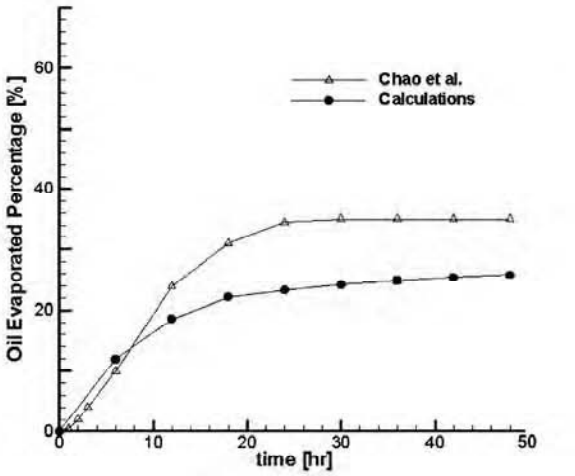

Fig. 14—Comparison of total evaporated oil (48 hours)

In Figures 14 and 15 a comparison between the total evaporated oil from the surface and oil slick thickness for time periods of 48 and 58 hours is made with Chao et al.'s work. This results show less amount of evaporation from the surface which is about 8%. From other hand it shows more oil slick thickness, due to the emulsification effects which have been considered in this work. In fact, in considering emulsification, oil disperses to water column and does not evaporate. In Fig. 16, a comparison of buoyancy effect for oil vertical dispersion with Lonin[24] results, is shown. It can be seen that, without buoyancy effect, oil droplets due to their mean diameters, have about 4-7 times more vertical dispersion in the water column. The Lonin's results show a 4 times more vertical dispersion. This difference is due to the consideration of evaporation, emulsification and dissolution in this work. Lonin[24] only used evaporation in his research. The presence of emulsification effect causes more vertical dispersion due to the effect of heavy components. Finally, regarding the buoyancy effect, calculations show a vertical dispersion in the water column twice as Lonin's prediction, while without buoyancy effect, the vertical dispersion is about 3.7 times of Lonin's.

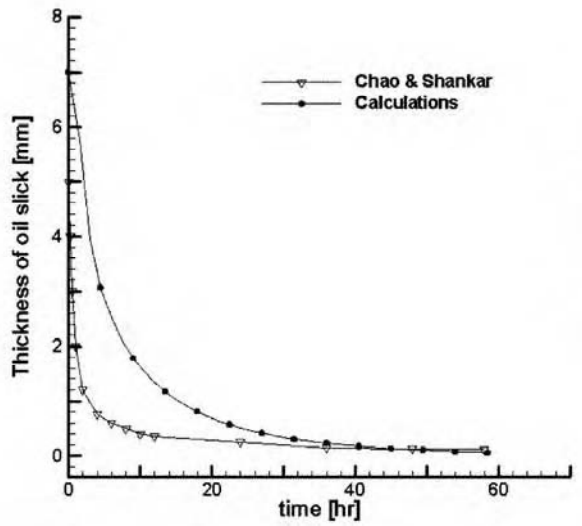

Fig. 15—Comparison of oil slick thickness

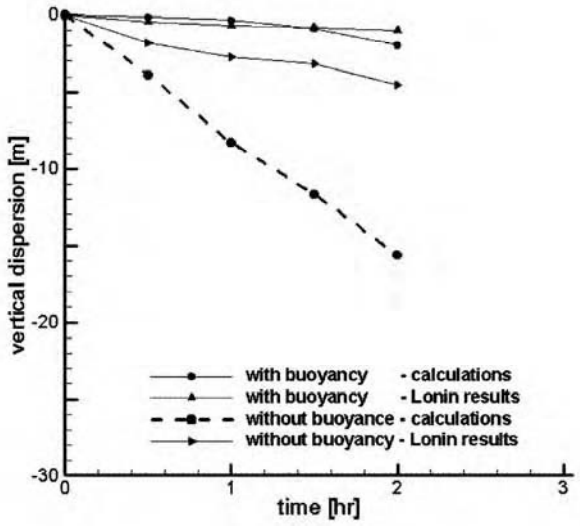

Fig. 16—Buoyancy effect on oil vertical dispersion

Conclusion

A model was developed to predict the trajectory of spilled oil and also to predict the oil slick thickness and slick surface area along its trajectory. Remaining oil volume on the surface, the evaporated oil, emulsified and dissoluted oil percentage and oil movement of a sample particle on the surface are the results of this prediction too. In horizontal spreading, surface spreading and horizontal dispersions are important and in decay processes, evaporation and emulsification are important and dissolution has a minor effect. Buoyancy effect and vertical turbulent variations are very important mechanisms for vertical movement of the oil in the water column. By means of the Kelvin wave theory concept, it has been justified that this new hydrodynamic calibration approach presents roughly better results in comparison with an alternative hydrodynamic model especially in the Persian Gulf. This improvement is not only towards a better estimation of the flow pattern in a simple manner, but also in a better presentation of a successful speed-up procedure. Horizontal and vertical dispersion coefficients were calibrated for the Persian Gulf and an artificial wind field was used to cover the lack of wind field time series. The present study infers, simple estimation for the flow pattern by Kelvin wave theory, capability of using an artificial wind field time series, calibration of dispersion coefficients and Langevin equation and an oil spill response and environmental impact assessment.

References

1 Spaulding M L, A state of the art review of oil spill trajectory and fate modeling, *J. of Oil and Chem. Pollut.,* 4(1988) 39-55.

2 Cekirge H M, Koch M & Long C, *State-of-the art techniques in oil spill modeling*, (Oil Spill Conference, USA, Library of Congress Catalog) 1995, pp. 67-72.

3 Lou A & Xi P, Prediction of oil spill track and study on its dispersion over the sea, *J. of Ocean, Univ. of Qingdao*, 4(1994) 477-480.

4 Lou A & Wang X, Studies on Monte-carlo method application for predicting marine oil spill diffusion, *J. of Mar. Sci.,* 5(2000) 7-10.

5 Korotenko K A, R M Mamedov & C N K Mooers, Prediction of the Dispersal of Oil Transport in the Caspian Sea Resulting from Continuous Release, *Spill Sci. & Tech. Bull.*, 5(2000) 323-339.

6 Chao X, Jothi Shankar N, Two and three dimensional oil spill model for coastal waters, *Ocean Eng.,* (2001) 1557-1573.

7 Wang S D, Shen Y M, Zheng Y H, Two dimensional numerical simulation for transport and fate of oil spills in seas, *Ocean Eng*., 32(2005) 1556-1571.

8 Hockney R W, Estwood J W, *Computer Simulation Using Particles*, (McGraw-Hill NY) 1981, pp. 640.

9 Ozmidov R V, *Diffusion of contaminants in the ocean Leningrad*, (Gidrometeoizdat) 1986.

10 Proctor R, Flather R A & Elliot A J, *Modeling tides and surface drift in the Arabian Gulf application to the Gulf oil spill*, (Continental Shelf Res.) 1994, pp. 531-545.

11 Zatzepa S N, *A mathematical model of oil spill dynamics on the sea surface*, PhD thesis, University of GOIN, Moscow, 1989.

12 Sebastiao P, Soares C G, Modeling the fate of oil spills at sea, *Spill Sci. and Tech. Bull.*, 2(1995) 121-132.

13 ASCE Task Committee on Modeling of Oil Spills of the Water Resources Engineering Div., State-of-the-art review of modeling transport and fate of oil spills, *J. of Hyd. Eng.,* 11(1996) 594-609.

14 Zamani A, Solomatine D P, Azimian A & Heemink A, Learning from data for wind–wave forecasting, *Ocean Eng.*, 35(2008) 953-962.

15 *Tides and Tidal streams*, *Admiralty manual of Hydrographic surveying*, Vol. 2, chap. 2, N. P. 134b(2) 1969.

16 Komen G J, Cavaleri, L, Donelan M, Hasselmann K, Hasselmann S, Janssen P A E M, *Dynamics and modeling of ocean waves*, (Cambridge university press) 1995, pp. 156.

17 Al-Rabeh, A.H., Estimating surface oil spill transport due to wind in the Arabian Gulf, *Ocean Eng.,* 5(1994) 461-465.

18 Delvigne G A L & Sweeney C E, Natural dispersion of oil, *Oil and Chem. Pollut.*, 4(1988) 281-310.

19 Zheng L & Yapa P D, Buoyant Velocity of Spherical and Non-Spherical Bubbles/ Droplets, *J. of Hyd. Eng., ASCE*, 11(2000) 852-855.

20 Chen F H & Yapa P D, Estimating the Oil Droplet Size Distributions in Deepwater Oil Spills, *J. of Hyd. Eng., ASCE*, 2(2007) 197-207.

21 Al-Rabeh A H, A Stochastic simulation model of oil spill fate and transport, *Applied Math. Modeling*, 13(1989) 322-329.

22 Lou A, Wu D & Wang X, Establishment of a 3D model for oil spill prediction, *J. of ocean, univ. of Qingdao*, (2001) 473-479.

23 Mackay D, Paterson S & Trudel K, *A mathematical model of oil spill behavior*, (environmental protection service, fisheries and environmental Canada) 1980.

24 Lonin S A, Lagrangian Model for Oil Spill Diffusion at Sea, *Spill Sci.& Tech. Bull.*, 5(1999) 331-336.

25 Cohen Y, Mackay D & Shiu W Y, Mass transfer rates between oil slicks and water, *J. of chem. Eng.*, 58(1980) 569-574.

26 Huang J C & Monastero F C, *Review of the state-of-the art of oil spill simulation models*, (final report submitted to the American Petroleum Institute, Raytheon Ocean System Co. East Providence, R.I.) 1982.

27 Fingas M, Fieldhouse B & Mullin J, *Studies of water-in-oil emulsions: stability Studies*, (Proceedings 20th Arctic and Marine Oil spill Program, AMOP, Technical Seminar, Vancouver, Environment Canada) 1997, pp. 211-263.

28 Fingas M, Fieldhouse B & Mullin J, *Studies of water-in-oil emulsions: energy threshold of emulsion formation*, (Proceedings, 22th Arctic and Marine Oil spill Program, AMOP, Technical Seminar, Calgary, Environment Canada) 1999, pp. 167-186.

29 Fingas M, Fieldhouse B, Lerouge L, Lane J & Mullin J, *Studies of water-in-oil emulsions: energy and work threshold as a function of temperature*, (Proceedings, 24th Arctic Marine Oil spill Program, technical Seminar, Edmonton, Alberta, Environment Canada) 2001, pp. 109-114.

30 Mackay D & Zagorski W, *Water-in oil emulsions: a stability hypothesis*, (Proceedings, 5th Arctic Marine Oil spill program, technical seminar, environment Canada) 1982, pp. 61-74.

31 Xie H, Yapa P D & Nakata K, Modeling Emulsification after an Oil Spill in the Sea, *J. of Mar. Sys.,* 68(2007) 489-506.